Geochemistry Geophysics Geosystems G3
AN ELECTRONIC JOURNAL OF THE EARTH SCIENCES
Published by AGU and the Geochemical Society

Article
Volume 5, Number 6
26 June 2004
Q06007, doi:10.1029/2004GC000702
ISSN: 1525-2027

Seafloor seismic monitoring of an active submarine volcano: Local seismicity at Vailulu'u Seamount, Samoa

J. G. Konter and H. Staudigel
Scripps Institution of Oceanography, University of California, San Diego, 9500 Gilman Drive, La Jolla, California 92093-0225, USA (jkonter@ucsd.edu)

S. R. Hart
Woods Hole Oceanographic Institution, MS 25, Woods Hole, Massachusetts 02543, USA

P. M. Shearer
Scripps Institution of Oceanography, University of California, San Diego, 9500 Gilman Drive, La Jolla, California 92093-0225, USA

[1] We deployed five ocean bottom hydrophones (OBHs) for a 1-year seismic monitoring study of Vailulu'u Seamount, the youngest and easternmost volcano in the Samoan Archipelago. Four instruments were placed on the summit crater rim at 600–700 m water depth, and one was placed inside the crater at 1000 m water depth. An analysis of the first 45 days of records shows a very large number of seismic events, 211 of them local. These events define a steady background activity of about four seismic events per day, increasing to about 10 events per day during a week of heightened seismic activity, which peaked at 40 events during 1 day. We identified 107 earthquakes, whose arrivals could be picked on all five stations and that are likely located within the seamount, based on their similar waveforms. Two linear trends are defined by 21 of these events. These are extremely well correlated and located, first downward then upward on a steeply inclined plane that is close to the axial plane of the southeast rift as it emerges from the main summit of Vailulu'u. These events resemble volcanotectonic earthquakes from subaerial volcanoes in displaying very coherent seismic waveforms and by showing systematic, narrowly defined progressions in hypocenter locations. We propose that these events reflect brittle rock failure due to magma redistribution in or near a central magma reservoir.

Components: 8510 words, 7 figures, 1 table, 1 animation.

Keywords: Samoa; Vailulu'u; volcano; seismic monitoring; volcanic activity; submarine.

Index Terms: 3025 Marine Geology and Geophysics: Marine seismics (0935); 7280 Seismology: Volcano seismology (8419); 8419 Volcanology: Eruption monitoring (7280).

Received 25 January 2004; **Revised** 16 April 2004; **Accepted** 10 May 2004; **Published** 26 June 2004.

Konter, J. G., H. Staudigel, S. R. Hart, and P. M. Shearer (2004), Seafloor seismic monitoring of an active submarine volcano: Local seismicity at Vailulu'u Seamount, Samoa, *Geochem. Geophys. Geosyst.*, *5*, Q06007, doi:10.1029/2004GC000702.

1. Introduction

[2] Seismology plays a central role in volcanology because it shows signals that are persistent and common, even if there are no current eruptions. This makes it an ideal tool to study submarine volcanoes, which are hard to monitor any other way. Recently, it has been shown that seafloor

seismic monitoring of submarine volcanoes is technically quite feasible [e.g., *Sohn et al.*, 1999]. This type of study shows it is now possible to monitor, identify and locate volcanic events within active submarine volcanoes. The recent establishment of National Ocean Bottom Seismology Instrumentation Pools (OBSIP, http://www.obsip.org) makes such work substantially less expensive and more accessible to the wider Earth science community.

[3] However, event location and characterization is still a step behind our understanding of subaerial volcanoes like Kilauea. On land, volcano seismology delivered the most detailed images of volcanic plumbing systems [*Ryan*, 1987], it helped us understand the intrusive growth of volcanoes [e.g., *Rubin and Gillard*, 1998], and it offers one of the most powerful tools for early warning and the prediction of volcanic eruptions. The success of seismology based volcano eruption prediction is illustrated in the 1991 Mt. Pinatubo eruption where massive numbers of casualties were prevented [*Punongbayan et al.*, 1996]. This makes it one of the best tools to monitor subaerial volcanoes.

[4] Seismology of submarine volcanoes has been successful at identifying volcanic eruptions through hydro-acoustic monitoring [e.g., *Fox et al.*, 1995, 2001] and through the deployment of seafloor seismometers on active volcanoes. The former has proven to be effective at monitoring the Juan de Fuca ridge and locating volcanic activity on it. For instance, *Fox et al.* [1995] reported on low-level seismic activity and harmonic tremor on Axial Volcano. Subsequently, Axial Volcano, Juan de Fuca Ridge, was monitored successfully 4 months by *Sohn et al.* [1999]. The authors located a substantial number of earthquakes with a distinct spatial progression that was attributed to volcanic–intrusive activity. They validated the utility of ocean bottom hydrophones (OBH) as an effective tool in submarine volcano seismology.

[5] In the case of seafloor seismometers, *Caplan-Auerbach and Duennebier* [2001b] studied the volcanically active Loihi seamount/Hawaii in 1998, but did not succeed in identifying local Loihi earthquakes, largely due to noise pollution from nearby lava flows entering the sea at Kilauea Volcano. However, with the help of island-based stations and one ocean bottom seismometer, these authors were able to locate a set of hypocenters of the 1996 earthquake swarm [*Caplan-Auerbach and Duennebier*, 2001a].

[6] In this paper, we report on a seafloor seismic monitoring study of Vailulu'u Seamount, the easternmost and still submarine, volcano at the leading edge of the Samoan Archipelago. The main goal of our study is to explore whether Vailulu'u Seamount is volcanically active and to understand the overall character and frequency of local seismic activity. Submarine seismology at Vailulu'u also may help us understand how submarine volcanoes work in comparison to the much better studied subaerial active volcanoes. In addition, these data may help us understand the hazard potential of Vailulu'u to navigation and Samoan coastal communities. Such an explosive volcanic hazard is quite realistic for Vailulu'u, because its summit is located at a water depth where other submarine volcanoes begin showing explosive volcanic activity (e.g., La Palma Seamount series [*Staudigel and Schmincke*, 1984]).

2. Seismology, Geology, and Hydrothermal Activity at Vailulu'u Seamount

[7] Vailulu'u Seamount (14°13′S, 169°04′W) is located at the eastern end of the Samoan chain, just off Ta'u Island with a summit at 600 m water depth, rising from an ocean depth of about 4800 m (Figures 1 and 2). This gives Vailulu'u a total height of over 4200 m, placing it into the size category of major isolated volcanoes on Earth, like Mt. Fuji, Etna, Mt. Hood, Pinatubo or Redoubt Volcano. However, it is much smaller than major volcanic islands that are made of several coalesced volcanoes, such as the Island of Hawaii. Vailulu'u is elongated with two main rift zones to the east and west, and a 2 km wide and 400 m deep crater at its summit. A minor, SE trending rift zone merges with the west rift at the highest summit of the volcano on the western side of the cratered summit (Figure 1) [*Hart et al.*, 2000].

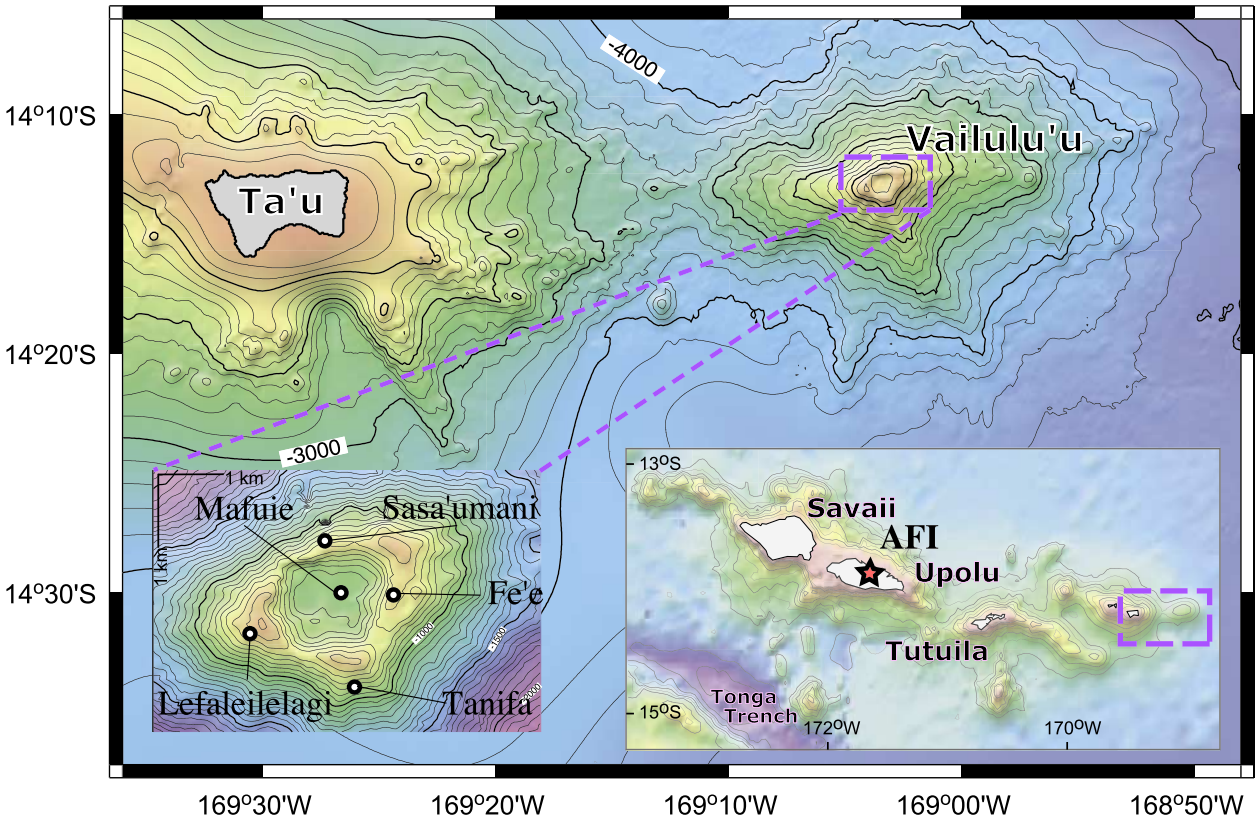

Figure 1. Bathymetry of Vailulu'u and its location east of Ta'u Island, on the eastern end of the Samoan Chain. The volcano ranges in depth from 4800 to 592 mbsl and has rifts to the east and west and a smaller one to the southeast. These rifts emerge from the three high points in the crater rim. The inset on the right shows the location of Vailulu'u and the whole Samoan chain with respect to the Tonga trench. The red star shows the location of the GSN station AFI. The inset on the left displays the area around the crater and the location of the OBHs (circles).

[8] Vailulu'u Seamount and the associated Samoan archipelago are located in a unique global tectonic setting, northeast of the Tonga Trench (Figure 2). The Tonga Trench defines a roughly north-south trending convergent plate boundary that, at its northern termination, turns into an east-west transform plate boundary. Tonga acts like a can opener that pries apart the Pacific plate: the southern section of the plate is subducted beneath the Tonga arc and the northern Pacific plate continues its path, sliding past the Tonga-Fiji-Lau Basin arc-back-arc region [e.g., *Bird*, 2003]. The Samoan archipelago is situated on the Pacific plate just north of Tonga (see Figures 1 and 2). The origin of the Samoan chain has been ascribed to either tension plate splitting [*Hawkins and Natland*, 1975], or more recently to a hotspot and possible rejuvenation by the faster moving trench corner [*Hart et al.*, 2000; S. R. Hart, et al., Genesis of the Western Samoa Seamount Province: Age, geochemical fingerprints and tectonics, submitted to *Earth and Planetary Science Letters*, 2004], based on the existence and location of Vailulu'u Seamount.

[9] The seismic activity in the region illustrates this tectonic setting (Figure 2): The northern Tonga Arc, Fiji and Lau Basin region is amongst the most seismically active areas in the world, with a large number of earthquakes in its lithosphere and upper mantle, with a planar array of deep earthquakes indicating the steep subduction of the Pacific plate (Figure 2). The Pacific plate, however, and underlying mantle to the north and east are practically devoid of earthquakes, except for one isolated cluster of relatively poorly located, shallow earthquakes beneath and northwest of Vailulu'u (Figure 2). This cluster of earthquakes occurred over a relatively short time period during

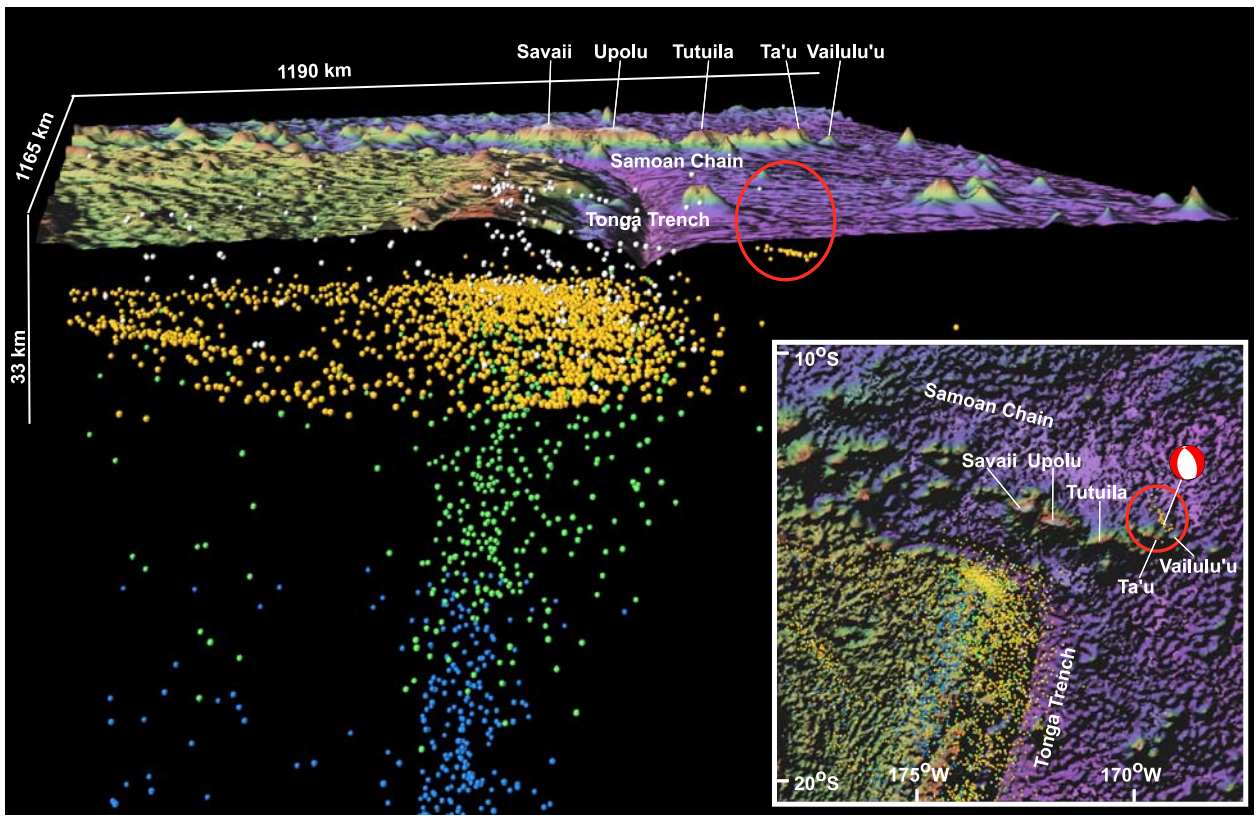

Figure 2. Three-dimensional view of the seismicity and bathymetry around Vailulu'u, including the Samoan chain and the northern edge of the Tonga trench. The colored dots show earthquake hypocenters (magnitudes 4 and higher) from the NEIC catalog (1973–2003) for this region. Hypocenters located up to 33 km depth are shown in white, at 33 km in yellow from 33–100 km in green and 100–200 km in blue. Earthquakes close to Vailulu'u are shown in the red oval, showing all but one in yellow. The depths of events in yellow are not meaningful as they are preset to a depth of 33 km. The only earthquake with a meaningful depth estimate in the NEIC catalogue is at 18 km depth, constrained by two pP picks (50 Hz data) about 75° away. The ISC review places this event at 35.2 ± 22.3 km, but neither depth estimate is sufficiently well known to relate this earthquake meaningfully to the data presented in this paper. The inset shows a map view of the same area, showing both the separation of Tonga events and the events near Vailulu'u and also showing a focal mechanism for the biggest event. Since the cluster is aligned with the NW-SE striking nodal plane, this is likely to be the fault plane.

9–29 January 1995 (M 4.2–4.9). However, even though it is poorly located and restricted to a rather small time interval, it is interesting to observe that these earthquakes are spatially well isolated from Tonga seismic activity, and therefore there is no seismic evidence that would link Vailulu'u or Samoa to the Tonga trench system. In addition, since they all appear to be similar in magnitude, it is likely that this represents an earthquake swarm associated with magmatic activity rather than a mainshock-aftershock sequence. Also, for one of these events a focal mechanism was determined (Harvard Centroid Moment Tensor, see also Figure 2), which indicates normal faulting. Notably, the swarm lines up with the 335° striking nodal plane, suggesting this to be the fault plane.

[10] Seismic activity near Vailulu'u was first recorded on 10 July 1973, by ocean acoustic monitoring indicating a series of major submarine explosions, motivating Rockne Hart Johnson to locate the volcano responsible for these events. He identified Vailulu'u (then named "Rockne") seamount as the most likely source for these submarine explosions [*Johnson*, 1984]. Direct evidence for volcanic activity, however, had to wait until the first detailed mapping and dredging of the seamount by the R/V *Melville*

Table 1. Hydrophone Deployments at Vailulu'u Seamount, Including Station Number, Instrument Name, the Location, Depth and the Total Period of Time, With Data Records Beginning 23 March 2000[a]

Station Number	Name	Latitude, °S	Longitude, °W	Deployment Depth, m	Sampling Frequency, Hz	Recording Period (Approximate), months
1	Lefaleilelagi	14°12.80′	169°3.27′	625	25	12
2	Fe'e	14°12.82′	169°2.83′	679	25	2
3	Tanifa	14°13.61′	169°3.16′	770	125	10
4	Sasa'umani	14°13.16′	169°4.15′	678	125	10
5	Mafuie	14°12.41′	169°3.49′	994	125	10

[a] Instruments are named after Polynesian gods, used in Figures 1 and 4. All instruments were deployed the same day, and their clocks were synchronized.

of Scripps Institution of Oceanography in March 1999 (Avon 2 and 3 cruises). These cruises demonstrated the cratered nature of Vailulu'u's summit, and recovered abundant unaltered volcanic glass in the summit region that indicates recent submarine volcanic activity.

[11] Some of the rocks were dated by *Hart et al.* [2000] using $^{210}Po/^{210}Pb$ and $^{210}Pb/^{226}Ra$ disequilibria, yielding ages of less than 5–30 years, overlapping in time with the 9–29 January 1995 seismic events. Encouraged by these data and facilitated by the recent startup of the SIO OBSIP facility, we were able to deploy five ocean bottom hydrophones (OBHs) on Vailulu'u. The main goal of this deployment was to establish whether or not this volcano is seismically active.

[12] For the actual deployment we used the U.S. Coast Guard Icebreaker Polar Star on its "Deep Freeze 2000" return leg from icebreaking duty in McMurdo Sound. During this cruise, a series of CTD-Nephelometer hydrocasts and subsequent water analyses offered strong chemical and physical evidence for hydrothermal venting [*Hart et al.*, 2000; *Staudigel et al.*, 2004]. These measurements set the stage for more detailed water column measurements including a dye release experiment during the "Deep Freeze 2001" OBH recovery aboard the USCG Icebreaker Polar Sea. This second round of water column measurements 12 months later confirmed persistent hydrothermal venting, provided two independent and nearly identical estimates for hydrothermal fluxes and substantially improved our understanding of how the hydrothermal systems interact with the ocean [*Hart et al.*, 2003; *Staudigel et al.*, 2004]. These combined lines of evidence offer robust evidence for substantial and enduring volcanic activity at Vailulu'u.

3. Seismic Monitoring Experiment at Vailulu'u Seamount

[13] We deployed five OBHs at Vailulu'u seamount for 1 year beginning late in March 2000 with a recovery in early April 2001. Four instruments were placed on the crater rim and one in the crater floor, with an array aperture of about 2.5 km (Figure 1). Four hydrophones were deployed by lowering them over the side of the icebreaker and one by drop from helicopter (Tanifa, Figure 1 and Table 1). All instrument locations were surveyed with detailed acoustic interrogation and GPS navigation before recovery using a small boat launched off the Polar Sea. All five instruments returned data, even though one instrument failed after 2 months of successful data recording.

[14] The OBHs that we used offer two choices for seismogram recording frequencies, 25 Hz or 125 Hz, with an expected battery life of 12 months or 6–8 months, respectively. These hydrophones have a flat frequency response between approximately 50 mHz and 30 Hz. Most of the seismic signals used in this paper are within 2–10 Hz, and thus 25 Hz is sufficient for identifying the major waveforms, but 125 Hz will make a more detailed analysis of the data possible, obviously at the expense of maximum instrument endurance. We chose 25 Hz for two instruments (Lefaleilelagi and Fe'e; Table 1), intending to record the whole time period of the deployment and 125 Hz for the

remaining three instruments, allowing for a more detailed analysis.

[15] The duration of our 1-year deployment was largely fixed by the deployment schedule of the Polar Class icebreakers. We did not limit the recording period of the instruments because our key goal was to capture any earthquakes over the maximum time possible. So we deliberately took the risk of running out of power in some of our instruments because event detection was a higher priority than our ability to correct for clock drift at the end of an experiment. One of the two 25 Hz instruments, Lefaleilelagi, recorded for the entire period of deployment, while Fe'e only recorded about 2 months of data. The clock drift for Lefaleilelagi was +1.25 s/year. The three remaining instruments, Tanifa, Sasa'umani and Mafuie lasted for about 10 months, longer than expected, but batteries expired before termination of the experiment and clock drift cannot be determined directly.

4. Seismic Signals and Noise

[16] Ocean floor hydrophones record acoustic signals from any sound sources emitting within their bandwidth, including solid Earth sources (local or distant earthquakes) as well as a range of sources from the ocean. Thus our ability to perform local seismic monitoring critically depends on distinguishing local signals from distant signals and from noise. We illustrate the potential sources of noise and signals in a set of spectrograms and their associated waveforms for two types of signals (Figure 3). This includes a local event and a T phase, both showing significant noise in the lower frequencies. Records from Mafuie were picked for this purpose, because this instrument rests on the crater floor at about 1000 m depth, and has the lowest noise levels.

[17] Overall it is quite apparent that ocean noise overwhelms signals at low frequencies, while signal-to-noise ratios are favorable at intermediate frequencies (2–10 Hz), and then worsen toward higher frequencies. In the low-frequency range ocean noise may include long-period gravity waves at frequencies lower than 0.02–0.03 Hz [*Babcock et al.*, 1994; *Webb*, 1998], while currents and turbulence in the seafloor boundary layer contribute to noise levels between 0.03–0.1 Hz [*Babcock et al.*, 1994; *Webb*, 1998]. Microseisms in the 0.1–5 Hz band provide the highest noise levels, where the longer period waves are Rayleigh waves resulting from large storms and the shorter periods are generated by more calm, wind-driven ocean waves [*Webb*, 1998]. *Caplan-Auerbach and Duennebier* [2001a] suggest that oceanic microseism noise occurs at frequencies below about 1.6 Hz. The intermediate frequency range from 5–10 Hz has relatively low noise levels, making it suitable for ocean bottom seismology [*Webb*, 1998]. However, any noise that is present in this range has been ascribed to wave breaking by *McCreery et al.* [1993]. Above 10 Hz the main source of noise is generated by ships (10–50 Hz [*Wenz*, 1962]), while the second source is marine mammals [*Pickard and Emery*, 1990].

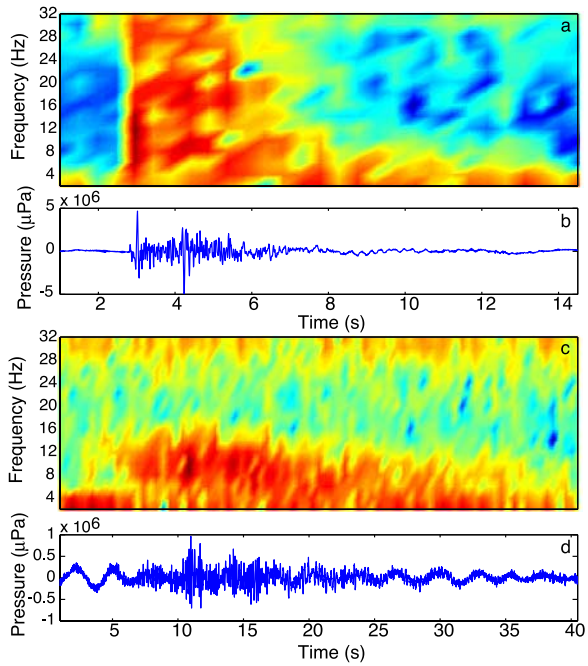

Figure 3. Example spectrograms and waveforms of a local event and a T phase (unfiltered data). (a and b) The local event shows significant energy above 10 Hz and a more impulsive arrival than (c and d) the T phase. The latter has a smaller range in frequency and is more emergent. Both spectrograms were constructed with a 0.5 s sliding window, running through the whole record shown next to each event.

[18] There is also a substantial seismic signal load from the oceans, in particular teleseismic acoustic phases (T phases) that have most of their power around 2–5 Hz (Figure 3) [*Leet*, 1951; *Leet et al.*, 1951]. These are normally characterized by emergent arrivals and long wave trains that may contain multiple peaks [*de Groot-Hedlin and Orcutt*, 1999]. The summit of Vailulu'u is located within the SOFAR channel, which transmits sound through the oceans with minimal power loss. Vailulu'u's crater rim array has a direct line of sight to almost the entire Pacific Rim, known to be one of the most seismically active regions on the planet. Thus a substantial T phase event load is expected in our seismic records.

[19] There are two basic types of (solid Earth) seismic signals that we might expect to detect with an OBH at Vailulu'u, including local events from within the volcano and underlying oceanic crust or teleseisms that may come from anywhere on Earth but most likely from the nearby Tonga Arc or transform plate boundaries. Volcano seismic events can be subdivided into high- and low-frequency events [e.g., *Lahr et al.*, 1994; *Chouet*, 1996]. The high-frequency events, with significant energy above 5 Hz, are associated with shear failure in the brittle volcanic edifice, commonly referred to as volcanotectonic (VT) events [*Power et al.*, 1994]. Low-frequency events can be either long-period (LP) events or harmonic tremor. The former have more emergent arrivals than small tectonic events and they show a peak frequency around 1–2.5 Hz [*Fehler and Chouet*, 1983]. Tremor, on the other hand, generally shows a harmonic signal over minutes to days. Notably, volcanic LP events display a similar range in energy as T phases. Especially these low-frequency signals overlap with the range of frequencies with high noise levels (below 2 Hz).

[20] We searched for signs of any of these volcano seismic events in the time between Julian day 85 and 131 (25 March to 10 May 2000). We focused on this time period because it is the time period for which all of the deployed instruments recorded high-quality data giving us the best opportunity to characterize and explore the causes of seismicity and to locate them. We reserved the remaining data in our 1–year time series for a separate study focusing on the frequency of events using the results of this study for recognition of seismic event types. We further focused our work in this paper on "VT events" at higher frequency, since other volcanic signals like tremor and LP events have to compete with high noise levels in the low-frequency range. After considering the various sources of noise and the main range of our signal, we applied a fourth-order Butterworth, 2–10 Hz band-pass filter, to improve the signal-to-noise ratio (e.g., Figure 3).

[21] In this filtered data, we observed three types of events. Both high-frequency, impulsive events with short (a few seconds long) codas and lower frequency, emergent events with minute long codas are present in the data sets. Also, four nonlocal body wave arrivals were found, whose arrival times agree well with a Tonga trench origin. In the following description of the data processing the main two types will be classified as local VT events and nonlocal T phases. Other types of volcanic signals were not observed in the records. However, preliminary analyses suggests that both these types of events continue to occur in a similar fashion throughout several months after these first 45 days.

[22] While processing the data with these two dominant signals, we focused on identification of local VT events. This was largely done by identifying and thereby eliminating all teleseismic events from global seismic catalogues, and by comparing our data to the Global Seismic Network (GSN) station on Western Samoa (AFI, red star in Figure 1). We predicted arrival times for teleseismic events including all catalogued events within 10° and all magnitude 4 and higher events outside 10°. For this, we calculated arc distances between catalogue locations (PDE, Preliminary Determinations of Epicenters, and CIT, California Institute of Technology) and OBH locations and estimated travel times for body waves with the IASP91 model (through the Matlab toolbox of the Antelope software package: http://www.brtt.com). T phase arrivals were estimated based on catalogued locations and approximate travel times calculated from arc distances and assuming the acoustic

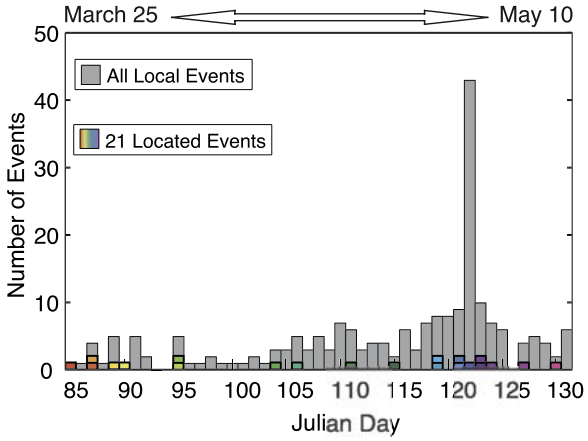

Figure 4. Histogram of all local seismic events in gray. The colored bars show the 21 best correlating events out of all recorded events coded from red for the first earthquake to purple for the last, and the same code is used for hypocenter locations in Figure 7. There is a clear peak in activity around day 122, which also shows a clustering of several of the best correlating events.

signals travel at approximately 1.5 km/s through the SOFAR channel. Most of the recorded events were found to agree reasonably with the predicted T phase arrival times whereby the most significant differences were identified for some distant and deep events. In addition, arrival times generally suggest velocities around 1.5 km/s, which suggests that they are likely not to be local volcanic signals (tremor or LP events), but instead T phases. It is interesting to note that most of the T phases appeared to have higher amplitudes on the crater rim than on the crater floor.

[23] After removal of the known four Tonga events and the T phases from our 45 day record, we identified 211 events with similar waveforms that are candidates for local VT events (see Figure 4). None of these events could be found in the records of the nearby GSN station AFI on Upolu Island (Figure 1), although AFI was not operational for some of this time. Out of the 211 events it was possible to pick arrival times on all stations for a subset of 107 events.

[24] Subsequently, these seismograms were cross-correlated to obtain more precise picks of first arrivals and better constrained hypocenter locations [e.g., *Got et al.*, 1994; *Shearer*, 1997; *Rubin et al.*, 1998; *Jones et al.*, 2001; *Rubin*, 2002]. The resulting cross-correlation coefficients only show a small group with similar numbers around 0.9 to 1. When sorted, the coefficients show a gradual increase to this cluster around 0.9 to 1 instead of a steep drop-off, a distribution that might be suggestive of just one local cluster of events within the volcano during this time period of 45 days.

[25] In order to study this cluster, we selected a subset of best correlated events, using a correlation coefficient >0.9 for waveforms at Mafuie. Since Mafuie has the best signal-to-noise ratio, not all the remaining events visually aligned as well on other stations. Therefore the cutoff was raised slightly above 0.9 at Mafuie until the remaining events lined up equally well on all stations. This resulting set consists of 21 events that we subsequently focused on for a detailed analysis. All of these 21 events display waveforms that are nearly identical for each station, but different between the stations (Figure 5). These well-correlated events give us a realistic opportunity to constrain the character of local seismic processes and relate them to volcano structure and volcanotectonic processes.

5. Timing and Location of Local VT Events

[26] We explored the periodicity of seismic activity on Vailulu'u in a time series of all of our 211 candidates for local events, plotting the number of events per day in Figure 4. Each event is represented by a gray box except for the 21 highly correlated events that are color coded for the time of their occurrence. There are about four earthquakes per day for the first 20 days of our time series, distributed relatively evenly with time. Between days 104 and 117, seismic activity appears to increase in intensity, still randomly but at a higher overall daily rate. Frequencies of earthquakes substantially increase between days 118 and 125, with 8 earthquakes per day, peaking on day 122 (1 May 2000) with over 40 events of which about 20 took place during approximately three hours, more than an order of magnitude above the background rate. The remaining time displays continued enhanced activity when compared with the first 20 days,

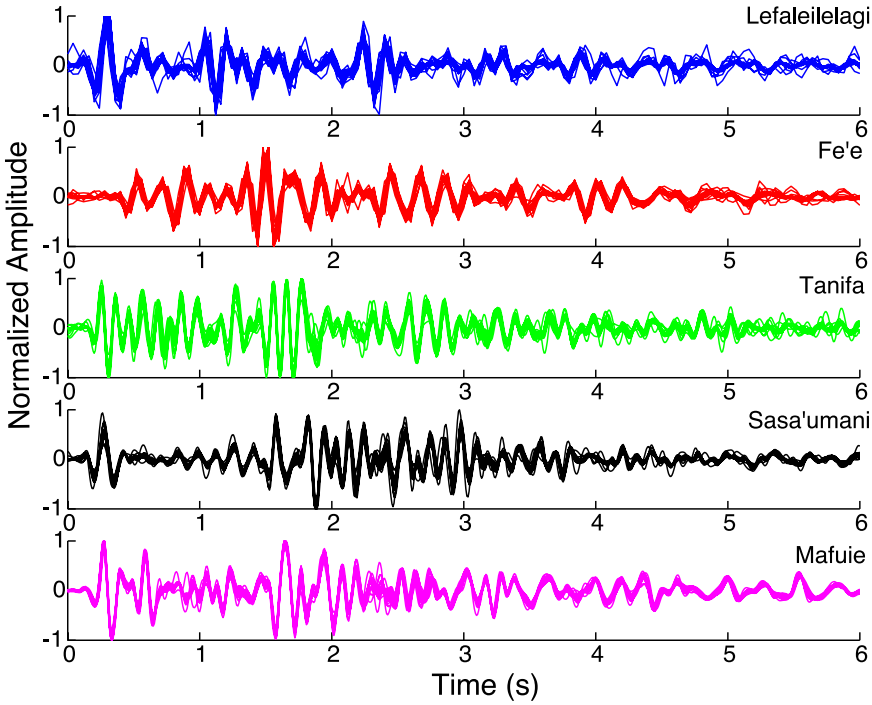

Figure 5. Waveforms for the 21 best correlating events are shown for each station. Lefaleilelagi and Fe'e show a less-perfect match, likely due to their lower sampling frequency. Tanifa, Sasa'umani and Mafuie show better correlations, with later peaks matching up to and beyond 6 s for Mafuie. This station is more shielded to acoustic phases by the crater rims around it, yielding lower noise levels. Last, the waveforms between stations are significantly different, suggesting heterogeneous structure within the volcano, since magnitudes are small.

but it is clearly less than the day 118–125 cluster. The 21 highly correlated events appear to be almost evenly distributed throughout this time series.

[27] Hypocenter locations of earthquakes can be estimated either through relative timing of the first P arrivals or by using P-S separation between stations. The latter does not produce stable locations in our records even for our best correlated 21 events, partly because hydrophones detect S wave arrivals only through a P wave conversion in water. This leaves us with the first P arrivals as our only choice. Hypocenter location estimates through first P arrivals, however, critically depend on the synchronization of the instrument clocks, which could be checked only for only one instrument, Lefaleilelagi.

[28] We made a first-order assessment for clock drift by comparing interevent times between different hydrophones. This assessment is straightforward when all earthquakes come from the same hypocenter, as is likely for our 21 best correlated events with nearly identical waveforms. The interevent time can be calculated as the difference of the first arrival times between events at a particular station and they should remain constant if all earthquakes come from the same place and if there is no instrument drift. This evaluation becomes more complicated if event locations are not the same for all earthquakes, because then arrival times will be different depending on the distance between earthquake and receiver. However, even in this case, interevent time differences between different seismic records should scatter around zero and should not change with time, unless the clock drifts. For our data set, we calculated interevent time differences for every instrument relative to Lefaleilelagi, which drifted 1.25 s/year. The resulting trends are nonlinear and within 0.1 s from zero for all instruments, indicating there is no significant clock drift relative to Lefaleilelagi over the first 45 days and that the events are not identical in

location. This allows us to ignore clock drift, at least to a first order.

[29] Hypocenter location estimates also require the calculation of travel times from the source to the receiver, which can only be realistically done with a reasonable velocity model of the seamount. Since there are no velocity data available for this seamount and the number of events to be located is small, we have to assume a velocity model that is derived from another seamount. Two such models may be considered: the model for Jasper Seamount [*Hammer et al.*, 1994] is likely to underestimate velocities in Vailulu'u, since the former has an extensive volcaniclastic cover. However, the model for the apparently less sediment covered Loihi shows even slower velocities [*Caplan-Auerbach and Duennebier*, 2001b]. Moreover, Loihi Seamount is a much smaller volcanic edifice, sitting on the flanks of Hawaii. Jasper Seamount, however, forms an isolated volcano, rising from the seafloor to about 600 mbsl, which makes it similar in size to Vailulu'u. Consequently, using a horizontally layered velocity model as in the one-dimensional model of Jasper Seamount [*Hammer et al.*, 1994] seems the most suitable assumption. This model has an approximately parabolic relationship of depth vs. P wave velocity, from approximately 2 km/s at the surface through 5 km/s at 2 km depth to about 6 km/s at 5 km depth.

[30] Using this velocity model, hypocenters were located with an adaptive migrating three-dimensional grid search algorithm, using first P arrivals. First a grid search over 10 × 10 × 10 km, with nodes every 100 m was performed for the minimum in variance of residuals (predicted-observed travel times). Subsequently, a second search was performed in a finer mesh grid around the first found minimum. This fine search was done over a 2 × 2 × 10 km grid, with nodes every 10 m horizontally and every 100 m vertically, whereby all grid searches followed standard procedures described by *Shearer* [1999]. We used the Jasper Seamount velocity model [*Hammer et al.*, 1994] to compute travel time residuals, using the calculated average velocity between each station and the depth of the grid node and the linear distance between them. Curved ray paths will change the travel times slightly. However, due to the short source-receiver distances the differences are far smaller than the residuals.

[31] The uncertainty in hypocenter locations, if done formally with a χ^2 approach [e.g., *Shearer*, 1999] likely overestimates the real uncertainty, due to the small number of stations. For this reason, we used a bootstrapping approach to determining errors in hypocenter locations. For this, we randomly adjusted arrival times of a synthetic event on all stations up to the maximum value of the highest observed residual (0.04 s) of the best fit locations. This adjustment and the subsequent event location procedure were repeated one hundred times yielding a bootstrapped location distribution in the form of a prolate ellipsoid (cigar shape). The axes of this ellipsoid have a 2σ of 533 m, 146 m and 55 m for the long axis (largely vertical), the horizontal axis and the remaining short axis (using the first as a representative event for this analysis).

[32] The hypocenters of our 21 events show two nearly linear arrays of events under the shallowest (western) summit and next to the northwestern pit crater (fit in Figure 6, locations in Figure 7 and Animation 1). The color-coding from Figure 4 suggests a temporal progression along these two trends. Since this migration in hypocenter locations covers a vertical range of about 1200 m, which is more than twice our bootstrapped error estimate of 533 m, these depths are statistically different. This implies the trend generally to the south-southeast must be significant, starting downward with red at 1300 m to 1800 m depth below the summit, and then upward to 600 m (in purple).

[33] We explored the quality of our hypocenter locations by calculating the travel time residuals between our best fit prediction and the actual travel time. Systematic nonzero offsets in these residuals may indicate local complexities in velocity structure and a systematic temporal trend may indicate a drifting clock. The origin time is unknown for these events; therefore the residuals were corrected by subtracting the average residual of all stations for a node from the residuals of that node. The subsequent residuals of the best fit locations show

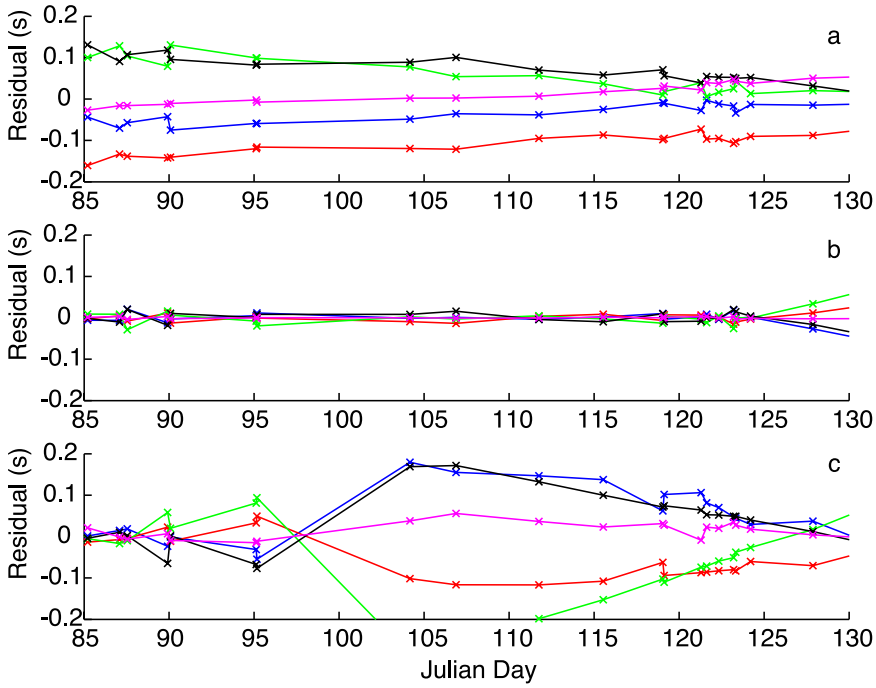

Figure 6. Residuals of travel times for all best locations against time of occurrence: predicted travel times minus the observations. (a) Residuals of all best locations located with the grid search. (b) Residuals of the iteratively corrected best fit locations. Corrections were made for nonzero mean (assumed to be station-specific velocity anomalies) and linear trends in residuals over time (assumed to be clock drift) visible in Figure 6a. Clearly, the fit of the corrected locations is significantly better. (c) Nonzero mean corrected residuals, assuming all events occurred in the same (first event) location. If clock drift was responsible for the apparent trend in locations, then the residuals at the first location for all events should show linear trends. Since these trends are nonlinear, individual locations are more likely (and provide a substantially better fit; see Figure 6b).

nonzero means and clear positive or negative trends versus time of occurrence (Figure 6a). Lefaleilelagi, Fe'e and Mafuie show a positive trend with time, while Tanifa and Sasa'umani are negative. These trends are probably not just due to the grid size, since 0.5 s in 45 days is far larger than possible by migration of locations between two grid nodes. The maximum grid node separation in a 10 m × 10 m × 100 m block is the diagonal distance across this block (approx. 101 m), which gives a maximum node separation of less than 0.1 s.

[34] We hypothesize that nonzero means in residuals are due to local velocity anomalies, while the trends may be due to clock drift. Assuming this is the case, we may correct the hypocenter locations iteratively by fitting a line to the temporal trend in the residuals (least squares fit). For every station, the mean value of this line relates to the local velocity anomalies, while the trend relates to possible clock drift. This least squares relation between residual and event occurrence is subsequently used to adjust the arrival times, by adding or subtracting the best fit value for every event. With these adjusted arrival times, the next iteration starts by finding corrected hypocenters. Iterations were stopped once the maximum corrections of the arrival times were smaller than 0.0075 s. After these corrections, the residuals are substantially reduced and show zero slope and zero mean (Figure 6b). This implies that the possible velocity anomalies and clock drift have been removed.

[35] These corrections define a similar pattern of hypocenter locations, shown as colored stars in Figure 7, with the same color-coding for event time. Depths range from 300 to 3500 m, starting at 900 and gradually moving deeper and then shallower again. Therefore our clock drift correction did not collapse the locations but rather moved them further apart.

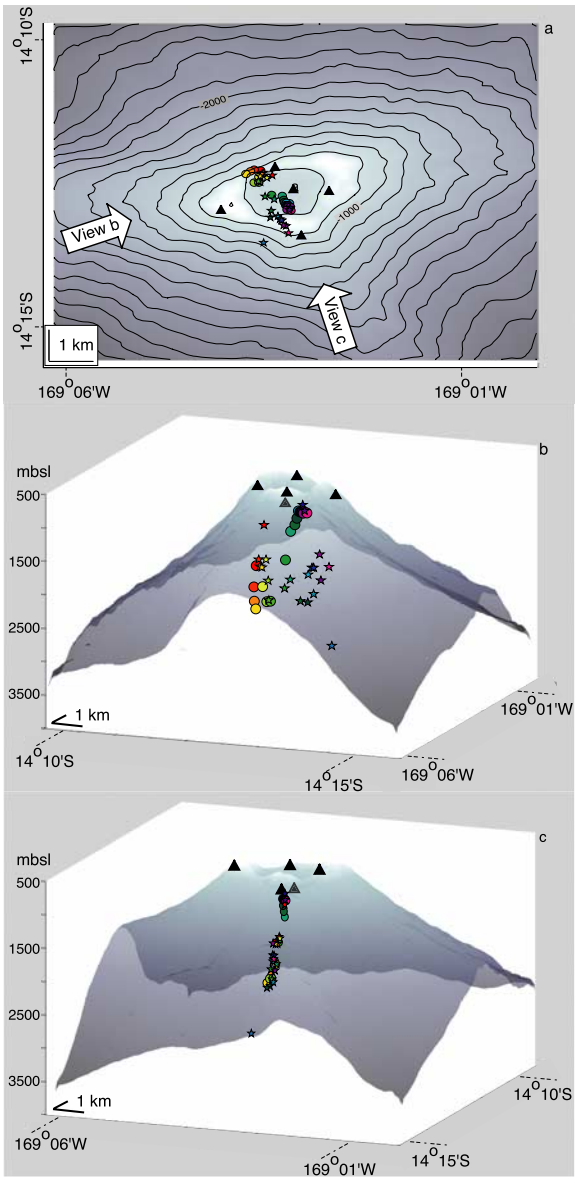

Figure 7. Hypocenters of the 21 best correlating events. The hypocenters found by the simple grid search are shown as circles, color coded as in Figure 3 according to time of occurrence. The stars show the same coding and represent the corrected locations. The black triangles represent the OBH locations. (a) Map view of the volcano and the hypocenters. The arrows show the direction of view for Figures 7b and 7c. (b and c) Three-dimensional perspective of the volcano. The viewpoint in Figure 7b is normal to the best fit plane through all locations, while the viewpoint in Figure 7c is parallel to it. These views display a semilinear trend in hypocenters for the not-corrected locations, a trend first down to the southeast, then up again in the same direction. The corrected locations are more planar than linear but still show a clear migration from northwest to southeast. The southwest dipping planar character of the hypocenter locations is well delineated.

[36] For this reason, we performed an additional test to explore what instrument drift would actually be needed to collapse the locations to one place. For this, we used the best fit location of the first located event, since this should be subject to virtually no (assumed linear) drift. Subsequently, we calculated the residuals for this solution and plotted them as a time series (Figure 6c). However, this stable, nonmoving hypocenter location causes residuals with a sinusoidal trend with time and slopes that may be as high as twice the observed clock drift of Lefaleilelagi (Figure 6c). Such residuals would indicate nonlinear and very large clock drifts that are very unlikely, and for this reason we reject clock drift as the main cause for the hypocenter migration in Vailulu'u.

[37] Thus we conclude from this discussion that there is indeed significant uncertainty in our data, but clock drift cannot be the main cause for the observed migration of hypocenters. Instead, we suggest that hypocenters move in a linear fashion, first down and then up, as indicated as color-coded stars in Figure 7. These two trends define a plane that has a surface exposure coinciding with the SE rift, at the crater rim fault in the SW portion of the crater (Figure 7a). Furthermore, we prefer the corrected locations, since these correspond to the smallest residuals that are corrected for possible three-dimensional velocity structure and clock drift.

6. Volcano Tectonic Events at Vailulu'u

[38] Volcano tectonic events at Vailulu'u may be caused by several processes, even though all VT events are ultimately caused by brittle failure of rock. Such brittle rock failure is generally brought about by stresses built up in the volcano by shifting magma or thermal cooling of a magma body [*Chouet*, 1996]. The most common tectonic processes, such as the postvolcanic or synvolcanic collapse of a volcano, are also ultimately caused by volcanic or intrusive processes that oversteepen the volcano slopes so they become subject to gravitationally driven failure. This latter process may be enhanced by weakening of the volcano structure by hydrothermal activity [*Lopez*

and Williams, 1993]. Purely plate tectonic processes are unlikely for Vailulu'u due to its intraplate setting. However, active volcanoes may also deform aseismically. For example, the South flank of Kilauea has been shown to slip by about 8 cm per year away from the massive Mauna Loa block against which it is buttressed [*Owen et al.*, 2000]. Such aseismic slip contributes to the overall deformation of a volcano, and may build up stress that could not be easily related to a well timed and located magmatic event. This all shows that the causes for brittle failure of rock in a volcano can be quite complex, and the true understanding of a volcano critically depends on a range of data and approaches, obtained over long monitoring periods. This applies to subaerial and submarine volcanoes.

[39] The 21 Vailulu'u seismic events studied here have great similarities with VT events from other volcanoes: they display very consistent waveforms, nearly identical for all earthquakes on a particular hydrophone, and the hypocenter locations cluster tightly and show systematic spatial trends. Such behavior is commonly observed at subaerial volcanoes, for instance Redoubt, Kilauea and Mt. Pinatubo. At Redoubt volcano, several sets of events with similar waveforms were found that form a linear trend of events along an almost vertical path [*Lahr et al.*, 1994]. The authors explain this trend as an area showing relaxation around several dikes and/or sills.

[40] A linear trend in similar VT events at Kilauea was interpreted to be associated with the stress concentration immediately above the deep rift body [*Rubin et al.*, 1998]. The authors found it likely that the ambient differential stress was only large enough to generate detectable earthquakes directly above the deep rift body (previously interpreted as a partially molten intrusive body [*Clague and Derlinger*, 1994; *Ryan*, 1988]) and not around the propagating tip of the 1983 dike. *Got et al.* [1994] identified 250 events, all with similar waveforms, arranged in a thin 100–200 m band at about 8 km depth beneath Kilauea volcano. This planar trend was interpreted as a fault plane representing the basal slip layer below the upper south flank of Kilauea volcano.

[41] Last, the preeruption seismicity at Mount Pinatubo showed two groups of seismic events: one shallow group (2–4 km) with a linear trend and a deeper group (3–5 km) with hypocenters defining a plane dipping at approximately 60° [*Jones et al.*, 2001]. The shallow linear trend was interpreted to form a pencil–shaped volume of seismicity directly above a magma body or partial melt zone, and the planar grouping was related to a fault also identified in an outcrop at the surface.

[42] VT events at Vailulu'u resemble in particular the planar group of events at Pinatubo. The two (corrected) linear trends at Vailulu'u form a planar surface with a strike of 343°, and a dip of 66° (dipping to SW). This is close to the probable fault plane of the 1995 swarm mentioned earlier (strike 335°), suggesting a preferential direction of fault activity. The surface exposure of this trend coincides roughly with the (minor) SE rift, as it emerges from the west rift closest to the highest summit of the volcano. Alternatively, this planar surface may be related to a fault associated with the collapse of the SW crater, or the collapse of the rather steep S flank of the volcano. In either case, the VT events coincide with a structural trend and planar features in the volcano that can be independently constrained from a geological interpretation of its topography. Furthermore, the similarities of Vailulu'u seismic data with that from subaerial volcanoes suggest that during the period of our study, internal deformation processes of this submarine volcano were not fundamentally different from processes in subaerial volcanoes from a wide range of settings.

[43] First arrivals of VT events can be either compressional or dilatational [e.g., *Rubin et al.*, 1998]. In the case of Vailulu'u, the waveforms of the 21 best correlating earthquakes show a downward (lower pressure, dilatational) first arrival. Given the small aperture of the array, it is likely that all instruments lie in the dilatational quadrant of the focal mechanisms for these events. This would suggest simple normal faulting (dilatational quadrant in the middle of the focal mechanism), implying these events are not likely to be associated with a propagating dike. The latter would produce only compressional arrivals [*Chouet and Julian*, 1985]. The normal faulting scenario leaves

us with two possibilities: continued collapse of the crater or southern steep side of the volcano, or deformation within the SE rift axial plane due to magma migration.

[44] It is somewhat speculative to identify a unique origin for the seismic events discussed. However, it is clear that these events do have a volcanotectonic origin, therefore demonstrating a significant level of volcanic activity at Vailulu'u. It is also quite obvious that the events display distinct clustering in linear arrays that first migrate down and then back up, with an overall dilatational character. The heightened activity is probably related to the redistribution of magma inside the volcano, because cooling would likely result in a more regular distribution of events. This shifting of magma between reservoirs may cause extensional earthquakes along a fault surface defined by our two linear trends. All of this is happening in a region of the volcano that is nearly directly below the highest point of the volcano, which is likely the region with the most significant shallow magma supply.

7. Conclusions

[45] Our results show that Vailulu'u is volcanically active and that our array of five hydrophones has been quite effective in monitoring an active submarine volcano. We quantified background levels of seismicity at about four earthquakes per day, with heightened activity by an order of magnitude observed on 2 May 2000. Our study also shows many parallels between seamount seismic activity and subaerial volcano activity, during the 45 days that were studied. This suggests that same internal processes that shape subaerial volcanoes, may also play a role in submarine volcanoes like Vailulu'u. The results from our seismic investigation are in agreement with other evidence supporting Vailulu'u's ongoing volcanic and hydrothermal activity. Its activity and proximity to nearby harbors make Vailulu'u an attractive natural laboratory for the study of active submarine volcanic processes.

Acknowledgments

[46] The bulk of this work was funded by NSF-OCE, in grants to HS and SRH and the OBSIP facility at Scripps. Five hydrophones were provided by the Scripps OBSIP facility within weeks of its startup. To make this deployment possible, Dave Willoughby, Chrispin Hollinshead, and Jeff Babcock overcame nearly impossible deadlines and logistics tasks for this very first OBSIP hydrophone deployment. Deployment and recovery was courtesy of the US Coast Guard Icebreakers Polar Star and Polar Sea and their enthusiastic crews including the first–ever helicopter deployment of an OBH. This manuscript includes many comments, suggestions and results from insightful discussions with Jeff Babcock, Bernard Chouet, Gabi Laske and Steve McNutt. We thank Paul Okubo and Del Bohnenstiehl for very thorough reviews that improved the manuscript greatly.

References

Babcock, J. M., B. A. Kirkendall, and J. A. Orcutt (1994), Relationships between ocean bottom noise and the environment, *Bull. Seismol. Soc. Am.*, *84*, 1991–2007.

Bird, P. (2003), An updated digital model of plate boundaries, *Geochem. Geophys. Geosyst.*, *4*(3), 1027, doi:10.1029/2001GC000252.

Caplan-Auerbach, J., and F. K. Duennebier (2001a), Seismic and acoustic signals detected at Lo'ihi Seamount by the Hawai'i Undersea Geo-Observatory, *Geochem. Geophys. Geosyst.*, *2*, Paper number 2000GC000113.

Caplan-Auerbach, J., and F. K. Duennebier (2001b), Seismicity and velocity structure of Loihi Seamount from the 1996 earthquake swarm, *Bull. Seismol. Soc. Am.*, *91*, 178–190.

Clague, D. A., and R. P. Derlinger (1994), Role of olivine cumulates in destabilizing the flanks of Hawaiian volcanoes, *Bull. Volcanol.*, *56*, 425–434.

Chouet, B. A. (1996), Long-period volcano seismicity: Its source and use in eruption forecasting, *Nature*, *380*, 309–316.

Chouet, B. A., and B. R. Julian (1985), Dynamics of an expanding fluid-filled crack, *J. Geophys. Res.*, *90*, 11,187–11,198.

de Groot-Hedlin, C. D., and J. A. Orcutt (1999), Synthesis of earthquake-generated T-waves, *Geophys. Res. Lett.*, *26*, 1227–1230.

Fehler, M., and B. A. Chouet (1983), Operation of a digital seismic network on Mount St Helens Volcano and observations of long-period seismic events that originate under the volcano, *Geophys. Res. Lett.*, *9*, 1017–1020.

Fox, C. G., W. E. Radford, R. P. Dziak, T.-K. Lau, H. Matsumotu, and A. E. Schreiner (1995), Acoustic detection of a seafloor spreading episode on the Juan de Fuca Ridge using military hydrophone arrays, *Geophys. Res. Lett.*, *22*, 131–134.

Fox, C. G., M. Haruyoshi, and A. L. Tai-Kwan (2001), Monitoring Pacific Ocean seismicity from an autonomous hydrophone array, *J. Geophys. Res.*, *106*, 4183–4206.

Got, J.-L., J. Fréchet, and F. W. Klein (1994), Deep fault plane geometry inferred from multiplet relative relocation beneath the south flank of Kilauea, *J. Geophys. Res.*, *99*, 15,375–15,386.

Hammer, P. T. C., L. M. Dorman, J. A. Hildebrand, and B. D. Cornuelle (1994), Jasper Seamount structure: Seafloor seismic refraction tomography, *J. Geophys. Res.*, *99*, 6731–6752.

Hart, S. R., et al. (2000), Vailulu'u undersea volcano: The New Samoa, *Geochem. Geophys. Geosyst.*, *1*, Paper number 2000GC000108.

Hart, S. R., H. Staudigel, R. Workman, A. A. P. Koppers, and A. P. Girard (2003), A fluorescein tracer release experiment in the hydrothermally active crater of Vailulu'u volcano, Samoa, *J. Geophys. Res.*, *108*(B8), 2377, doi:10.1029/2002JB001902.

Hawkins, J. W., and J. H. Natland (1975), Nephelinites and basanites of the Samoan linear volcanic chain: Their possible tectonic significance, *Earth Planet. Sci. Lett.*, *24*, 427–439.

Johnson, R. H. (1984), Exploration of three submarine volcanoes in the South Pacific, in *On Research and Exploration Projects Supported by the National Geographic Society, for Which an Initial Grant or Continuing Support Was Provided in the Year 1975*, edited by P. H. Oehser, J. S. Lea, and N. L. Pomars, *Res. Rep. Natl. Geogr. Soc.*, *16*, 405–420.

Jones, P. J., C. H. Thurber, and W. J. Lutter (2001), High-precision location of pre-eruption seismicity at Mount Pinatubo, Philippines, 30 May–3 June, 1991, *Phys. Earth Planet. Inter.*, *123*, 221–232.

Lahr, J. C., B. A. Chouet, C. D. Stephens, J. A. Power, and R. A. Page (1994), Earthquake classification, location, and error analysis in a volcanic environment: Implications for the magmatic system of the 1989–1990 eruptions at Redoubt Volcano, Alaska, *J. Volcanol. Geotherm. Res.*, *62*, 137–151.

Leet, L. D. (1951), Discussion of "Proposed use of the T phase in tsunami warning systems", *Bull. Seismol. Soc. Am.*, *41*, 165–167.

Leet, L. D., L. Linehan, and P. R. Berger (1951), Investigation of the T-phase, *Bull. Seismol. Soc. Am.*, *41*, 123–141.

Lopez, D. L., and S. N. Williams (1993), Catastrophic volcanic collapse: Relation to hydrothermal processes, *Science*, *260*, 1794–1796.

McCreery, C. S., F. K. Duennebier, and G. H. Sutton (1993), Correlation of deep ocean noise (0.4–20 Hz) with wind, and the Holu spectrum—A worldwide constant, *J. Acoust. Soc. Am.*, *93*, 2639–2648.

Owen, S., P. Segall, M. Lisowski, A. Miklius, R. Denlinger, and M. Sako (2000), Rapid deformation of Kilauea Volcano: Global Positioning System measurements between 1990 and 1996, *J. Geophys. Res.*, *105*, 18,983–18,998.

Pickard, G. L., and W. J. Emery (1990), *Descriptive Physical Oceanography*, 320 pp., Pergamon, New York.

Power, J. P., J. C. Lahr, R. A. Page, B. A. Chouet, C. D. Stephens, D. H. Harlow, T. L. Murray, and J. N. Davies (1994), Seismic evolution of the 1989–1990 eruption sequence of Redoubt Volcano, Alaska, *J. Volcanol. Geotherm. Res.*, *62*, 69–94.

Punongbayan, R. S., C. G. Newhall, M. L. P. Bautista, D. Garcia, D. H. Harlow, R. P. Hoblitt, J. P. Sabit, and R. U. Solidum (1996), Eruption hazard assessment and warnings, in *Fire and Mud: Eruptions and Lahars of Mount Pinatubo, Philippines*, edited by C. G. Newhall and R. S. Punongbayan, pp. 67–85, Univ. of Wash. Press, Seattle.

Rubin, A. M. (2002), Using repeating earthquakes to correct high-precision earthquake catalogs for time-dependent station delays, *Bull. Seismol. Soc. Am.*, *92*, 1647–1659.

Rubin, A. M., and D. Gillard (1998), Dike-induced earthquakes: Theoretical considerations, *J. Geophys. Res.*, *103*, 10,017–10,030.

Rubin, A. M., D. Gillard, and J.-L. Got (1998), A reinterpretation of seismicity associated with the January 983 dike intrusion at Kilauea Volcano, Hawaii, *J. Geophys. Res.*, *103*, 10,003–10,015.

Ryan, M. P. (1987), Elasticity and contractancy of Hawaiian olivine tholeiite and its role in the stability and structural evolution of subcaldera magma reservoirs and rift systems, in *Volcanism in Hawaii*, edited by R. W. Decker, T. L. Wright, and P. H. Stauffer, *U.S. Geol. Surv. Prof. Pap.*, *1350*, 1395–1447.

Ryan, M. P. (1988), The mechanics and three-dimensional internal structure of active magmatic systems: Kilauea Volcano, Hawaii, *J. Geophys. Res.*, *93*, 4213–4248.

Shearer, P. M. (1997), Improving local earthquake locations using the L1 norm and waveform cross-correlation: Application to the Whittier Narrow, California, aftershock sequence, *J. Geophys. Res.*, *102*, 8269–8283.

Shearer, P. M. (1999), *Introduction to Seismology*, 260 pp., Cambridge Univ. Press, New York.

Sohn, R. A., W. C. Crawford, and S. C. Webb (1999), Local seismicity following the 1998 eruption of Axial Volcano, *Geophys. Res. Lett.*, *26*, 3433–3436.

Staudigel, H., and H.-U. Schmincke (1984), The Pliocene seamount series of La Palma/Canary Islands, *J. Geophys. Res.*, *89*, 11,195–11,215.

Staudigel, H., S. R. Hart, A. Koppers, C. Constable, R. Workman, M. Kurz, and E. T. Baker (2004), Hydrothermal Venting at Vailulu'u Seamount: The Smoking End of the Samoan Chain, *Geochem. Geophys. Geosyst.*, *5*, Q02002, doi:10.1029/2003GC000610.

Webb, S. C. (1998), Broadband seismology and noise under the ocean, *Rev. Geophys.*, *36*, 105–142.

Wenz, G. M. (1962), Acoustic ambient noise in the ocean: Spectra and sources, *J. Acoust. Soc. Am.*, *34*, 1936–1956.